NASA TECHNICAL MEMORANDUM

NASA TM X-2483

NASA TM X-2483

ANALYSIS OF LOSS-OF-COOLANT ACCIDENT FOR A FAST-SPECTRUM LITHIUM-COOLED NUCLEAR REACTOR FOR SPACE-POWER APPLICATIONS

by George E. Turney, Edward J. Petrik, and Arthur W. Kieffer

Lewis Research Center
Cleveland, Ohio 44135

NATIONAL AERONAUTICS AND SPACE ADMINISTRATION • WASHINGTON, D. C. • JANUARY 1972

1. Report No.	2. Government Accession No.	3. Recipient's Catalog No.
NASA TM X-2483		

4. Title and Subtitle	5. Report Date
ANALYSIS OF LOSS-OF-COOLANT ACCIDENT FOR A FAST-SPECTRUM LITHIUM-COOLED NUCLEAR REACTOR FOR SPACE-POWER APPLICATIONS	January 1972
	6. Performing Organization Code

7. Author(s)	8. Performing Organization Report No.
George E. Turney, Edward J. Petrik, and Arthur W. Kieffer	E-6571
	10. Work Unit No. 112-27

9. Performing Organization Name and Address	11. Contract or Grant No.
Lewis Research Center National Aeronautics and Space Administration Cleveland, Ohio 44135	
	13. Type of Report and Period Covered
12. Sponsoring Agency Name and Address	Technical Memorandum
National Aeronautics and Space Administration Washington, D.C. 20546	14. Sponsoring Agency Code

15. Supplementary Notes

16. Abstract

A two-dimensional, transient, heat-transfer analysis was made to determine the temperature response in the core of a conceptual space-power nuclear reactor following a total loss of reactor coolant. With loss of coolant from the reactor, the controlling mode of heat transfer is thermal radiation. In one of the schemes considered for removing decay heat from the core, it was assumed that the 4π shield which surrounds the core acts as a constant-temperature sink (temperature, 700 K (1260° R)) for absorption of thermal radiation from the core. Results based on this scheme of heat removal show that melting of fuel in the core is possible only when the emissivity of the heat-radiating surfaces in the core is less than about 0.40. In another scheme for removing the afterheat, the core centerline fuel pin was replaced by a redundant, constant-temperature, coolant channel. Based on an emissivity of 0.20 for all material surfaces in the core, the calculated maximum fuel temperature for this scheme of heat removal was 2840 K (5100° R), or about 90 K (160° R) less than the melting temperature of the UN fuel.

17. Key Words (Suggested by Author(s))	18. Distribution Statement
Loss-of-coolant accident Space-power reactor	Unclassified - unlimited

19. Security Classif. (of this report)	20. Security Classif. (of this page)	21. No. of Pages	22. Price*
Unclassified	Unclassified	35	$3.00

* For sale by the National Technical Information Service, Springfield, Virginia 22151

ANALYSIS OF LOSS-OF-COOLANT ACCIDENT FOR A FAST-SPECTRUM LITHIUM-COOLED NUCLEAR REACTOR FOR SPACE-POWER APPLICATIONS

by George E. Turney, Edward J. Petrik, and Arthur W. Kieffer

Lewis Research Center

SUMMARY

A two-dimensional, transient, heat-transfer analysis was made to determine the temperature response in the core of a conceptual space-power nuclear reactor following a total loss of reactor coolant. With loss of coolant from the reactor, the controlling mode of heat transfer is thermal radiation.

In one of the schemes considered for removing decay heat from the core, it was assumed that the 4π shield which surrounds the core acts as a constant-temperature sink (temperature, 700 K (1260° R)) for absorption of thermal radiation from the core. Results based on this scheme of decay heat removal show that the surface emissivity has a significant effect on the temperatures in the core. With an emissivity of 0.20, the core centerline fuel pin reached the melting temperature of UN (2923 K, or 5260° R) at about 1900 seconds after the loss-of-coolant accident. And with emissivity values of 0.40 and 0.80, the maximum fuel-pin temperatures were 2820 K (5080° R) and 2355 K (4240° R), respectively. Thus for emissivity values greater than about 0.40, thermal radiation to only the surrounding 4π shield is sufficient to prevent the fuel from reaching its melting point following a loss of coolant.

In another scheme for removing decay heat, the centerline fuel pin was replaced by a redundant coolant channel. With this arrangement, decay heat is transferred to both the redundant coolant channel and the 4π radiation shield. A constant temperature of 1222 K (2200° R) was assumed for the redundant coolant channel. Based on an emissivity value of 0.20 for all core materials, the calculated maximum fuel temperature for this scheme of heat removal was 2840 K (5100° R), or about 90 K (160° R) less than the melting temperature of uranium nitride (UN). Hence, it appears that a single coolant channel at the center of the core is sufficient to prevent fuel melting, even with an emissivity value as low as 0.20.

INTRODUCTION

Our nation's future space missions will require systems capable of delivering large amounts of electric power. To meet these future requirements, the Lewis Research Center has been working on a technology program aimed at the design of an advanced, high-powered, nuclear Brayton space powerplant. The heat source being considered for this advanced space powerplant is a compact, fast-spectrum, nuclear reactor. The basic design requirements for the reactor are that it produce 2.17 megawatts thermal power and that it operate continuously for 50 000 hours. In this conceptual space powerplant, the heat generated by the reactor is removed by liquid lithium which circulates continuously through a closed primary flow loop. The primary loop of this system is thermally coupled to one or more complete inert-gas Brayton power conversion loops. Neutronic design information for this fast-spectrum reactor is presented in reference 1; and the operating characteristics of the primary flow loop of this system are described in reference 2.

An important area which must be considered in the overall design of this system is the analysis of potential failures and/or system malfunctions. A preliminary analysis of several possible accidents in this system is reported by Davison (ref. 3). Of the many types of malfunctions and/or failures possible, one of the most serious is that which results from a complete loss of coolant in the reactor primary flow loop. With loss of coolant from the core, all heat interchange between the fuel, interior core structure, reflector, pressure vessel, and reactor shield is by radiation. For a failure of this type, we would like to know the temperature response of the fuel pins inside the core and also the conditions under which melting of fuel in the core is possible.

Two separate schemes for removing heat from the core were considered. In one scheme, we assumed that the radiation shield which surrounds the core acts as a constant-temperature sink for the absorption of heat transferred from the core. In the other scheme, the centerline fuel pin in the core was replaced by a redundant coolant channel. With this arrangement, there are two sinks for absorption of reactor heat: one at the center of the cylindrically shaped core, and the other outside the core (i.e., the surrounding radiation shield).

In order to investigate the loss-of-coolant accident for these two schemes of heat removal, a two-dimensional, transient, heat-transfer analysis was made. From the analysis, we determined the temperature response of the fuel pins inside the core and the transient temperature distribution throughout the core. The analysis was made by using the Chrysler Improved Numerical Differencing Analyzer for 3rd Generation Computers (CINDA-3G) digital computer program (ref. 4). The results of this study and a description of the thermal network model used to represent the core are presented in this report.

DESCRIPTION OF REACTOR

The reference design for this fast-spectrum reactor has 247 cylindrical fuel pins, each with an outside diameter of 1.905 centimeters (0.750 in.) and a length of 37.6 centimeters (14.8 in.). Figure 1 is a schematic of the reactor core design.

The main body of the core has 181 fuel pins arranged symmetrically in a six-pointed star shape. Another 66 fuel pins are in the six control drums just outside the main body of the core. Figure 2 shows a cross-sectional view of the fast-spectrum reactor core.

The fuel pins in the core contain cylindrically shaped uranium nitride (UN) pellets which are covered with a tungsten liner and encased in a T-111 (Ta-8W-2Hf) cladding. The interior of each fuel pellet has a central void which provides space for fission gas containment and fuel swelling. Figure 3 shows the arrangement of UN pellets in the present fuel-pin design.

The fuel pins in the core are cooled by lithium which flows through annular passages formed by the outside surfaces of the fuel pins and the inside surfaces of concentric T-111 tubes which surround the fuel pins. The surrounding T-111 tubes form a honeycomb structure; the tubes in this structure have an inside diameter of 2.11 centimeters (0.83 in.) and a wall thickness of 0.025 centimeter (0.010 in.).

The reactor thermal power is regulated by six control drums which, when rotated, move fuel (or a T-111 neutron absorber) near or away from the main body of the core. Each control drum has 11 fuel pins, a reflector of TZM (Mo-0.5Ti-0.08Zr), and a T-111 neutron absorber. Between the control drums near the periphery of the core is a fixed reflector of TZM. The pressure vessel surrounding the core is T-111 with a wall thickness of 0.625 centimeter (0.250 in.).

In the conceptual system design, the entire pressure vessel is surrounded with a radiation shield (4π type) consisting of alternate layers of tungsten and lithium-6 hydride.

As indicated in figure 2, the fuel pins are grouped into three zones. Fuel enrichment for each zone is the same, that is, 93.2 atomic percent of the uranium is the 235-isotope (U^{235}). However, the diameter of the central void in the fuel pellets (and consequently the volume fraction of UN) is different for each zone. Figure 4 shows a cross section of a fuel pin, along with dimensions of the pins in each of the three fuel zones.

The design-point operating conditions of the primary flow loop which are relevant to this study are listed in table I.

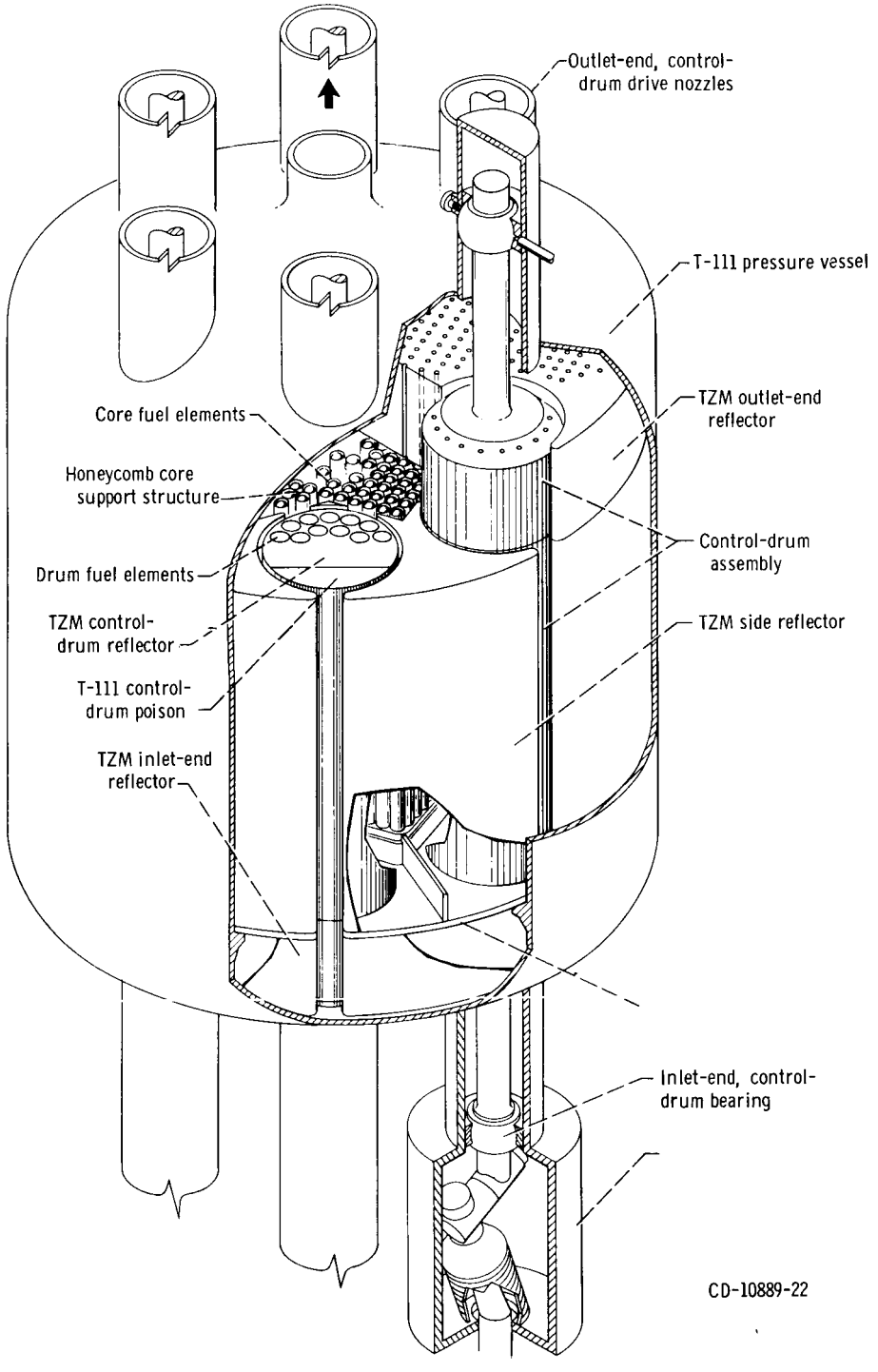

Figure 1. - Schematic of fast-spectrum, space-power reactor.

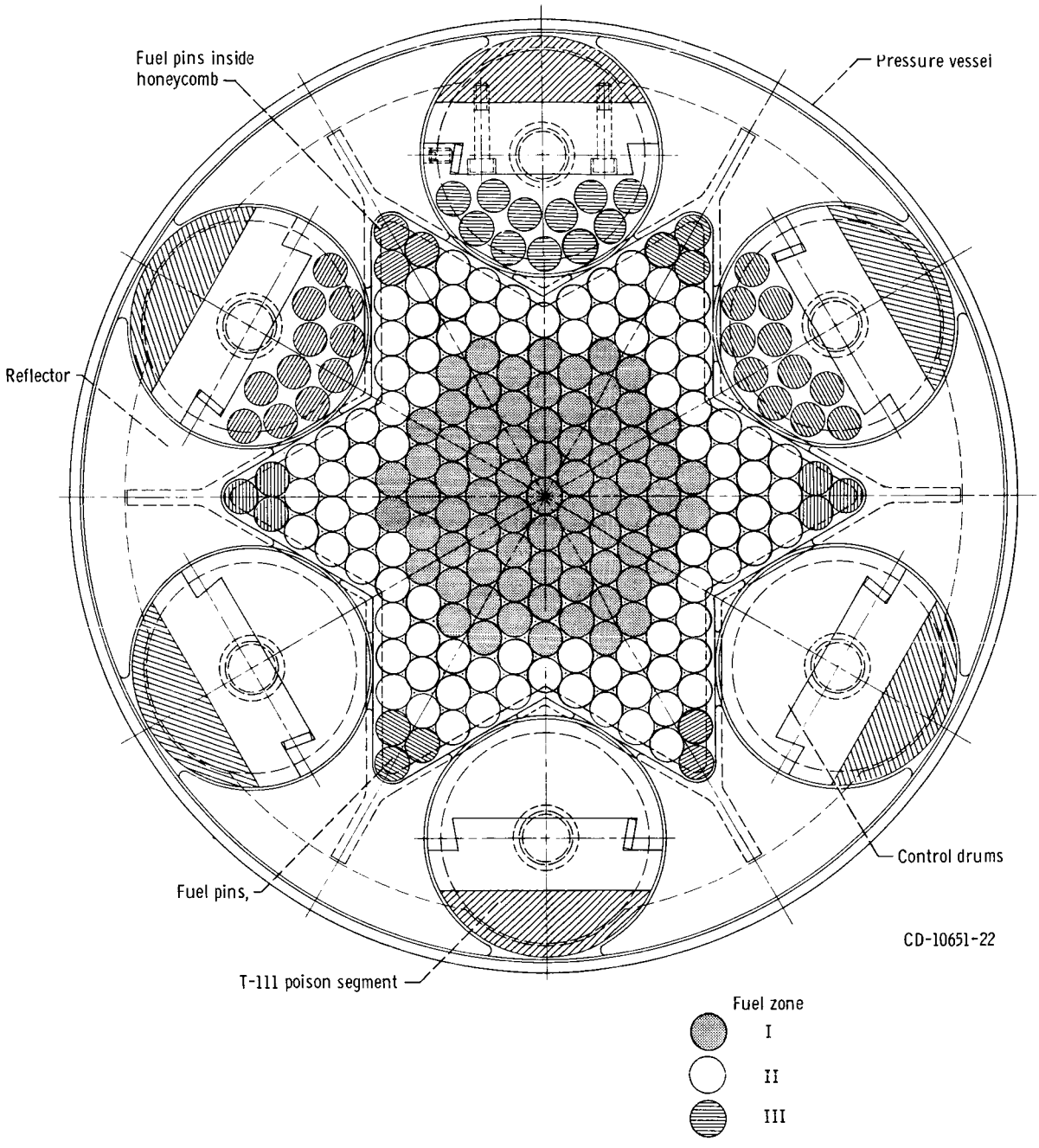

Figure 2. - Cross section of fast-spectrum, space-power reactor core.

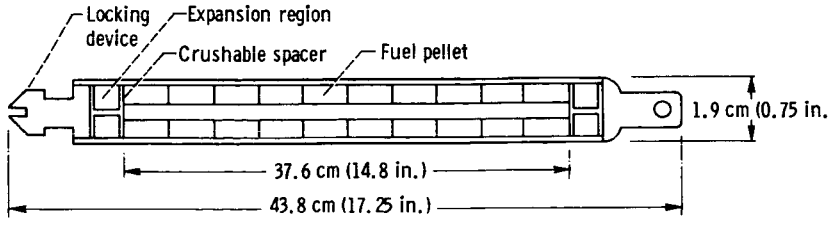

Figure 3. - Fuel-pin design for fast-spectrum, space-power reactor.

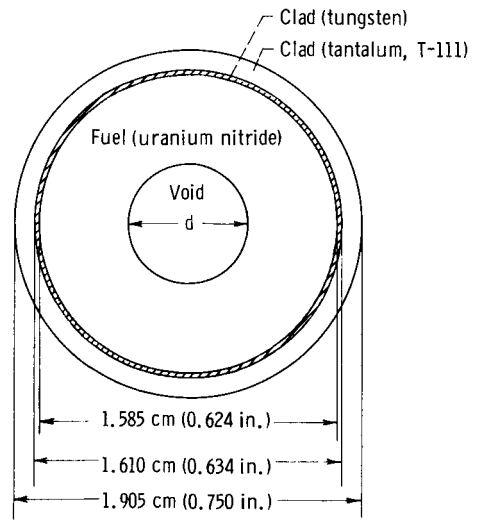

Fuel zone	Void diameter, d		Number of pins per zone
	cm	in.	
I	0.762	0.300	73
II	.678	.267	90
III	.480	.189	84

Figure 4. - Cross section of fuel pin and fuel-pin dimensions for the three fuel zones.

TABLE I. - DESIGN-POINT OPERATING CONDITIONS

Reactor thermal power, MW	2.17
Lithium temperature at reactor inlet, K (^{O}R)	1167(2100)
Lithium temperature at reactor outlet, K (^{O}R)	1222(2200)
Lithium flow rate, kg/sec (lbm/sec)	9.39(20.7)

ANALYSIS

General Considerations

If a break occurs in either the reactor pressure vessel or one of the primary-loop flow lines, the entire inventory of lithium coolant would be lost from the primary loop. Based on the design lithium flow rate (table I) and the inventory of lithium in the core, such a failure could result in the core being completely voided of lithium in less than 0.5 second.

In all likelihood a complete loss of coolant from the primary flow loop will render the system permanently inoperable. That is, it is unlikely that a failure of this type could be corrected in space and the system returned to normal operation. Therefore, the primary concern associated with the loss-of-coolant accident in this space-power reactor is to prevent the fuel from melting and possibly recombining to form a supercritical assembly.

In the event of a loss of reactor coolant, it is desirable that the reactor undergo an immediate (scram) shutdown. We have assumed, in the analytical treatment of this problem, that loss of coolant and shutdown of the reactor occur simultaneously. Hence, all heat generated in the core following a loss of coolant is decay heat - resulting from fission product decay, fissions by delayed neutrons, and radioactive emission due to parasitic absorption of neutrons.

The magnitude of the decay heat generation rate in the core following shutdown depends primarily on (1) the reactor's initial operating power level and (2) the period of time during which the reactor was in operation before the shutdown. To prevent melting of fuel in the core, a significant fraction of the decay heat must be transferred by thermal radiation from the core.

As stated in the INTRODUCTION, we investigated two separate schemes for removing decay power from the core following a total loss of reactor coolant. In one scheme we assumed that the 4π radiation shield which surrounds the core acts as a single, constant-temperature sink for heat transfer from the core. With this single thermal sink, heat is transferred radially outward from the interior of the core to the surrounding radiation shield. In the other scheme for removing decay power, the centerline fuel pin in the core was replaced by a redundant, constant-temperature coolant channel. With this arrangement, there are two thermal sinks for absorption of reactor decay heat. And decay heat generated in the fuel is transferred to both the redundant centerline coolant channel and the 4π radiation shield which surrounds the core.

Analytical Model of Core

The heat interchange process which takes place in the core following a loss of coolant was considered to be two-dimensional. Figure 5 is a sketch of the model used to represent the core for the transient heat-transfer analysis. It is a 30° sector of the core cross section with unit axial depth. The sides of the 30° sector model are adiabatic boundaries, and the control drums are assumed to be in their full-out (shutdown) position.

As indicated in figure 5, the 30° sector model is divided into a number of finite volume elements, each of which is represented by a nodal point. The boundaries of these volume elements are indicated by dashed lines. A total of 230 nodal points are used to describe the 30° sector model of the core. The breakdown of nodal points in this model is as follows: In the main body of the core, 96 nodes represent the fuel pins, and another 96 nodes represent the T-111 honeycomb tubes. In the control drum half, seven nodes describe the fuel pins, and 15 additional nodes describe the TZM and T-111 mater-

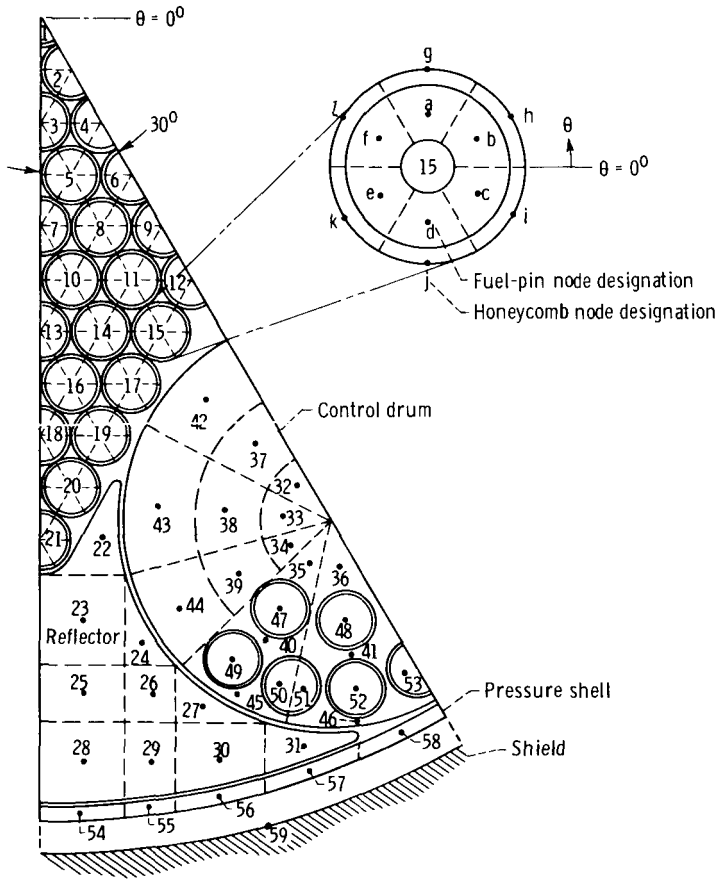

Figure 5. - Model for two-dimensional heat-transfer analysis of core following loss of coolant.

ial volumes. The TZM fixed reflector region has 10 nodes, and the T-111 pressure shell has five nodes. The radiation shield which surrounds the core is represented by a single node.

From figure 5, we see that each fuel pin in the core main body is divided by radial lines into a number of truncated, pie-shaped volume elements. And each of these volume elements, consisting of UN fuel, tungsten cladding, and T-111 cladding, is represented by a single nodal point. The individual nodal points associated with each fuel pin and each surrounding honeycomb tube in the main body of the core are designated by a number and letter. The identification scheme is illustrated in figure 5 for fuel pin 15. Thus, node e of fuel pin 15 represents the volume element of that fuel pin which extends from $\theta = \pi$ to $\theta = 4\pi/3$. Similarly, node k represents the honeycomb tube volume element which extends from $\theta = \pi$ to $\theta = 4\pi/3$.

For this analysis, we assumed the heat source for the fuel pins to be distributed uniformly throughout the UN fuel, the tungsten cladding, and the T-111 cladding. (This assumption was necessary since only one radial node was used for each fuel-pin volume element.) Based on this assumption, the nodal points in the fuel pins were positioned to coincide with the location of the mean radial temperature in the fuel-pin volume elements. The resulting radial locations of nodal points in the fuel pins of fuel zones I, II,

TABLE II. - RADIAL LOCATION OF NODES IN FUEL PINS

Fuel zone	Nodal location (radial distance from fuel-pin centerline)	
	cm	in.
I	0.673	0.265
II	.663	.261
III	.640	.252

and III are given in table II. The nodal points in all other volume elements were assumed to be at the geometric center (i.e., the centroid of area) of the elements.

The CINDA-3G thermal analyzer code (ref. 4) uses an electrical circuit model to represent the thermal network of the physical problem. And the equations which describe the thermal network are analogous to those which describe an equivalent electrical circuit. The thermal capacitances assigned to the nodes and the thermal resistances between nodes are represented by so-called "lumped-parameters." These lumped-parameters of resistance and capacitance form a resistance-capacitance thermal network. And the set of differential equations which describe the behavior of the thermal

network are solved simultaneously by an iterative technique. For this study we used the CINDA-3G execution subroutine called CNFRWD.

Analytical Assumptions and Input Data

The major assumptions used in the analysis of the loss-of-coolant accident are as follows:

(1) The initial temperature of the core (i.e., the temperature of fuel, cladding, interior core structure, reflector, and pressure vessel) is 1222 K (2200^{o} R). This is the approximate average design operating temperature of the core.

(2) The temperature of the radiation shield which surrounds the core remains constant at 700 K (1260^{o} R) following the loss of coolant. (The radiation shield acts as a sink for absorption of thermal radiation leaving the core.) This temperature is the approximate average design operating value for the radiation shield.

(3) The loss of coolant from the core is instantaneous and complete. Consequently, the transient phenomena associated with the loss of coolant process was not considered.

(4) All heat interchange between material surfaces in the core is by thermal radiation.

(5) The reactor is operated at design power for 1 year prior to the loss-of-coolant accident. And the reactor decay power used in the analysis was based on this design power operating period.

(6) For those calculations made with a redundant coolant channel at the center of the core, we assumed that this channel acted as an additional sink, and its temperature remains constant at 1222 K (2200^{o} R) following the loss-of-coolant accident.

In order to solve the thermal network equations, we must specify the initial conditions, the boundary conditions, and the heating rate in each fuel node. The initial conditions (i.e., the starting temperatures of all nodal points) are given by assumption (1). And the boundary conditions are given by assumptions (2) and (6).

The heating rate in each fuel node decays with time after the loss of coolant. As stated in the section General Considerations, we have assumed in the analysis of this problem that the reactor is shut down concurrently with the loss of coolant and that all heat generated in the core following the loss of coolant is decay heat.

Figure 6 shows the ratio of reactor decay power to design power against time after reactor shutdown. The data in this figure are based on the assumption that the reactor is operated at design power for a period of 1 year before shutdown. (As stated by assumption (5) in this section, the decay power used in this analysis was based on a design power operating period of 1 year prior to shutdown.)

The fuel-pin power factors (i.e., the local-to-average power ratios among the fuel pins) following 1 year of continuous design power operation are shown in figure 7. From

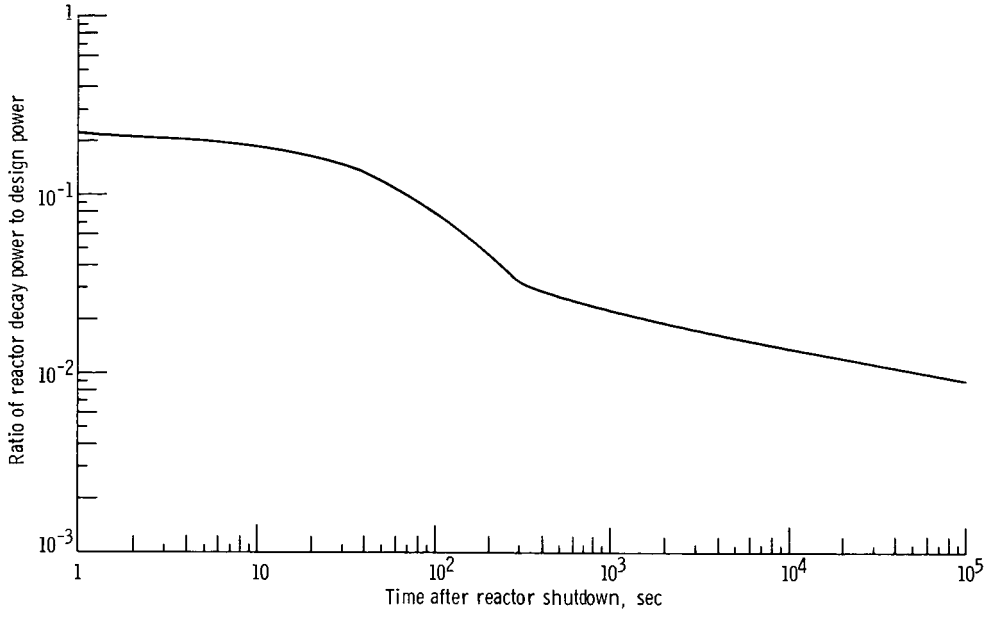

Figure 6. - Ratio of reactor decay power to design power against time after shutdown. Reactor operating time at design power before shutdown, 1 year.

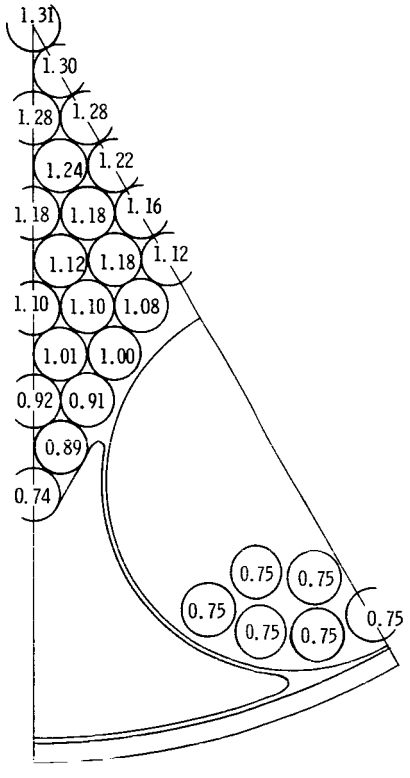

Figure 7. - Fuel-pin power factors (local-to-average power ratios) following 1 year of continuous design power operation.

the fuel-pin power factors (fig. 7) and the decay power data (fig. 6), the time-dependent heating rate for each fuel pin was determined as follows:

$$\begin{pmatrix}\text{Fuel-pin heating}\\ \text{rate at time } \theta\end{pmatrix} = \left(\frac{\text{Reactor design power}}{\text{Number of fuel pins in reactor}}\right) \times \begin{pmatrix}\text{Ratio of reactor decay}\\ \text{power to design power}\\ \text{at time } \theta\end{pmatrix} \times (\text{Fuel-pin power factor}) \qquad (1)$$

Similarily, the time-dependent heating rate in each fuel-pin node was computed as the product of the fuel-pin heating rate (eq. (1)) and the volume fraction of the fuel pin associated with the fuel-pin node.

The thermophysical materials properties used in this study were assumed to be constant and independent of temperature. The values used for the specific heats and thermal conductivities are listed in table III. The data in table III were taken from the references indicated and were evaluated at a temperature of 1922 K (3460° R).

Two kinds of nodes, diffusion and boundary, were used in the thermal network representation of the 30° sector model of the core. Each constant-temperature heat sink was represented by a single boundary node. All other nodes in the 30° sector model were diffusion nodes. Each diffusion node has a thermal capacitance associated with it, which permits storage of thermal energy. The thermal capacitance of a diffusion node is defined as the product of mass associated with the node and the specific heat (i.e., ρVC_p). (All symbols are defined in the appendix.)

Two types of thermal conductances were used in the network equations, namely

TABLE III. - THERMOPHYSICAL PROPERTIES

Material	Specific heat		Thermal conductivity	
	$\frac{\text{kW-sec}}{(\text{kg})(\text{K})}$	$\frac{\text{Btu}}{(\text{lbm})(^{\circ}\text{R})}$	$\frac{\text{kW}}{(\text{m})(\text{K})}$	$\frac{\text{Btu}}{(\text{sec})(\text{ft})(^{\circ}\text{R})}$
T-111[a]	17.1	0.041	0.0606	0.0097
UN[b]	27.7	.066	.0303	.0049
Tungsten[c]	16.8	.040	.1038	.0167
TZM[d]	29.3	.070	.0900	.0144

[a]Ref. 5.
[b]Ref. 6.
[c]Ref. 7.
[d]Ref. 8.

conduction and radiation. The conductance between conductor nodes G_C is defined as the inverse of the thermal resistance between nodes; that is,

$$G_C = \frac{kA}{l} \tag{2}$$

Radiation conductance does not have an equivalent inverse-resistance connotation. Rather, the radiation conductance between any two nodes designated as α and β in the 30^O sector model is denoted by $G_{R,\alpha\rightarrow\beta}$ and is defined as

$$G_{R,\alpha\rightarrow\beta} = \sigma A_{s,\alpha}\left[\frac{1}{\frac{1}{\epsilon_\alpha} + \frac{A_{s,\alpha}}{A_{s,\beta}}\left(\frac{1}{\epsilon_\beta} - 1\right)}\right] F_{\alpha\rightarrow\beta} \tag{3}$$

The thermal capacitance, conductor conductance, and radiation conductance represent the lumped parameters which are input to the CINDA-3G program.

Analytical Procedure

The equations which describe the thermal response of all nodes in the 30^O sector model are formulated from the basic energy equation. That is, for any node designated α in the 30^O sector model we can write

$$\begin{pmatrix}\text{Rate of change in}\\ \text{internal energy}\\ \text{of node } \alpha\end{pmatrix} = \begin{pmatrix}\text{Rate of net heat interchange by}\\ \text{conduction between node } \alpha\\ \text{and adjacent conduction nodes}\end{pmatrix}$$

$$+ \begin{pmatrix}\text{Rate of net heat interchange by}\\ \text{radiation between node } \alpha\\ \text{and adjacent radiation nodes}\end{pmatrix} + \begin{pmatrix}\text{Rate of heat generation in}\\ \text{the volume represented}\\ \text{by node } \alpha\end{pmatrix} \tag{4}$$

In the paragraphs which follow, we describe how equation (4) is applied to determine the temperature response of both a typical fuel-pin node and a typical node in the T-111 honeycomb structure.

Consider, for example, a cluster of three fuel pins and honeycomb tubes with nodal designations, as shown in figure 8. The thermal resistance network for the fuel-pin node e is depicted in figure 9. With reference to figure 9, the energy balance for node e can be written as follows:

$$\rho_e V_e C_{p,e} \frac{\Delta T_e}{\Delta \theta} = \left[G_{C,f\to e}(T_f - T_e) + G_{C,d\to e}(T_d - T_e)\right] + \left[G_{R,j\to e}(T_j^4 - T_e^4) + G_{R,l\to e}(T_l^4 - T_e^4) + G_{R,k\to e}(T_k^4 - T_e^4)\right] + (q_e'''V_e) \tag{5}$$

The change in temperature of fuel-pin node e with respect to time is obtained by rearranging equation (5); that is,

$$\frac{\Delta T_e}{\Delta \theta} = \frac{1}{\rho_e V_e C_{p,e}} \left[G_{C,f\to e}(T_f - T_e) + G_{C,d\to e}(T_d - T_e) + G_{R,j\to e}(T_j^4 - T_e^4) + G_{R,l\to e}(T_l^4 - T_e^4) + G_{R,k\to e}(T_k^4 - T_e^4) + q_e'''V_e\right] \tag{6}$$

Now consider a typical node in the honeycomb tube, such as node k in figure 8. The thermal resistance network for the honeycomb tube nodal point k is shown in figure 10. Applying equation (4) to nodal point k (which has no internal heat source) we have

$$\rho_k V_k C_{p,k} \frac{\Delta T_k}{\Delta \theta} = G_{C,l\to k}(T_l - T_k) + G_{C,j\to k}(T_j - T_k) + G_{R,l\to k}(T_l^4 - T_k^4) + G_{R,f\to k}(T_f^4 - T_k^4) + G_{R,e\to k}(T_e^4 - T_k^4) + G_{R,d\to k}(T_d^4 - T_k^4) + G_{R,j\to k}(T_j^4 - T_k^4) + G_{R,i\to k}(T_i^4 - T_k^4) + G_{R,g\to k}(T_g^4 - T_k^4) \tag{7}$$

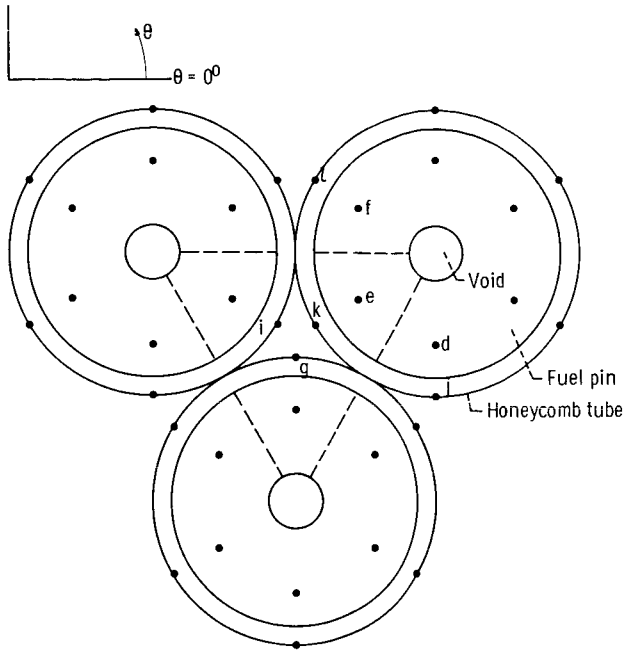

Figure 8. - Cluster of three fuel pins and honeycomb tubes with nodal points.

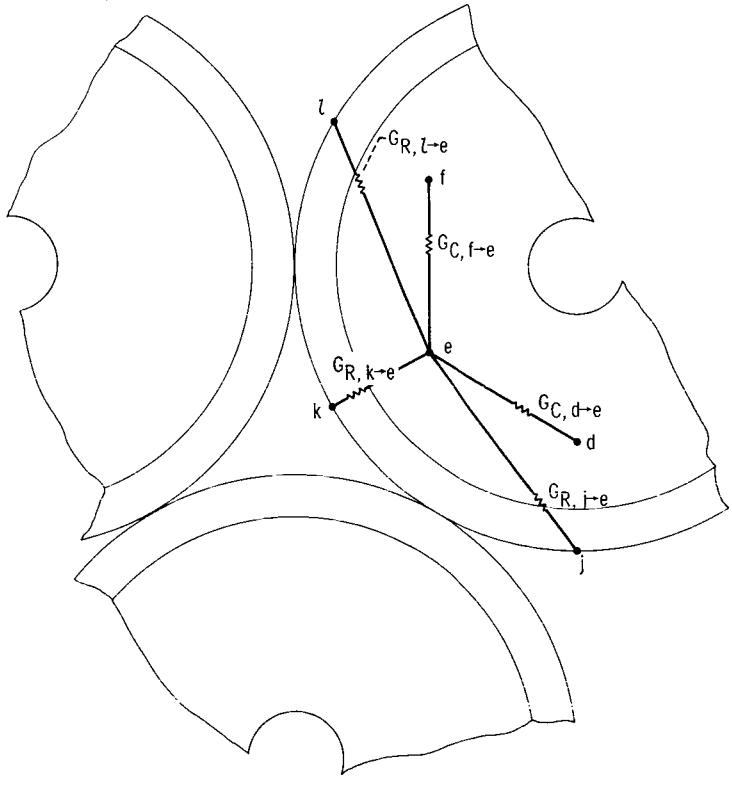

Figure 9. - Thermal resistance network for fuel-pin nodal point e.

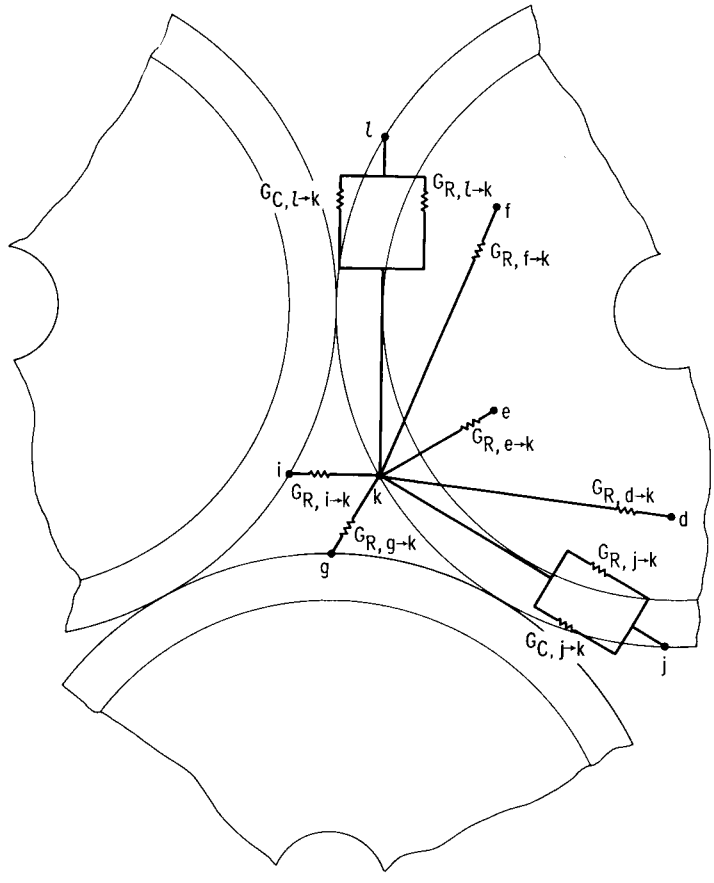

Figure 10. - Thermal resistance network for honeycomb tube nodal point k.

Similarly, the change in temperature of node k with respect to time is

$$\frac{\Delta T_k}{\Delta\theta} = \frac{1}{\rho_k V_k C_{p,k}} \left[G_{C,l\to k}(T_l - T_k) + G_{C,j\to k}(T_j - T_k) + G_{R,l\to k}(T_l^4 - T_k^4) \right.$$

$$+ G_{R,f\to k}(T_f^4 - T_k^4) + G_{R,e\to k}(T_e^4 - T_k^4) + G_{R,d\to k}(T_d^4 - T_k^4) + G_{R,j\to k}(T_j^4 - T_k^4)$$

$$\left. + G_{R,i\to k}(T_i^4 - T_k^4) + G_{R,g\to k}(T_g^4 - T_k^4) \right] \tag{8}$$

Relations similar to equations (6) and (8) describe the thermal response of each node in the 30^0 sector model of the core.

The CINDA-3G program computes the temperature change with respect to time of each node in the thermal network. As stated in the section Analytical Model of Core,

we used the CINDA-3G forward difference subroutine called CNFRWD to determine the time rate of change in temperature of each node in the network. The size of the time step (i.e., the value of $\Delta\theta$) used in the simultaneous solution of the thermal network equations is defined by a stability criteria formulation in the CNFRWD subroutine. For the time period $\Delta\theta$, the temperature change with respect to time of any node is

$$\frac{\Delta T}{\Delta \theta} = \frac{T_{\theta_2} - T_{\theta_1}}{\theta_2 - \theta_1} \tag{9}$$

And the temperature of any node at time θ_2 is related to the node temperature at the preceding time, θ_1, by the expression

$$T_{\theta_2} = T_{\theta_1} + \Delta T \tag{10}$$

The basic assumption used in this loss-of-coolant analysis is that all heat interchange between surfaces in the core is by thermal radiation. Because thermal radiation is the governing mode of heat transfer, the surface emissivity has a significant effect on the thermal response of the core.

The published values of emissivity for the materials in the core show wide variances. Because of these reported variations, we considered three different values of emissivity for the loss-of-coolant analysis, namely, 0.20, 0.40, and 0.80.

All radiating surfaces in the core were assumed to have the same emissivity. And a separate analysis was made for each of these three values of emissivity.

RESULTS AND DISCUSSION

As we have stated, two different schemes were considered for removing decay heat from the core following a total loss of reactor coolant. For each of these schemes, we determined the temperature response of all nodes in the 30° sector model of the core. But a description of the temperature-time history of all nodes is beyond the scope and ambitions of this report. Therefore, in what follows, we shall confine our discussion to the temperature response of the fuel pins which are located in the main body of the core.

First, we will describe results for the scheme in which the 4π shield which surrounds the core is considered as a single, constant-temperature sink for absorption of heat transferred from the core. Then, we will describe results for the second scheme,

in which a redundant coolant channel at the center of the core is used as a thermal sink in conjunction with the surrounding 4π radiation shield.

Scheme I - Decay Heat Absorption by Only the Surrounding 4π Radiation Shield

For this scheme of decay heat rejection, the direction of heat transfer is radially from the interior of the core to the surrounding 4π radiation shield. The radiation shield temperature is assumed to remain constant at 700 K (1260° R) following the loss of coolant.

Temperature response of core centerline fuel pin. - The centerline fuel pin (fuel pin 1 of fig. 5) has the largest power factor and also the largest overall resistance to radiation heat transfer. Thus, with a complete loss of reactor coolant and with radiation as the controlling mode of heat transfer, the centerline fuel pin reaches the highest temperature of any fuel pin in the core.

Figure 11 shows the temperature response of the centerline fuel pin for surface emissivities of 0.20, 0.40, and 0.80. From this figure we see that with an emissivity of 0.20 the centerline fuel pin reaches the melting point of UN at approximately 1900 seconds after the loss of coolant. In figure 11, the temperature response curve for the 0.20 emissivity is extrapolated (shown dashed) beyond the fuel melting point. It should

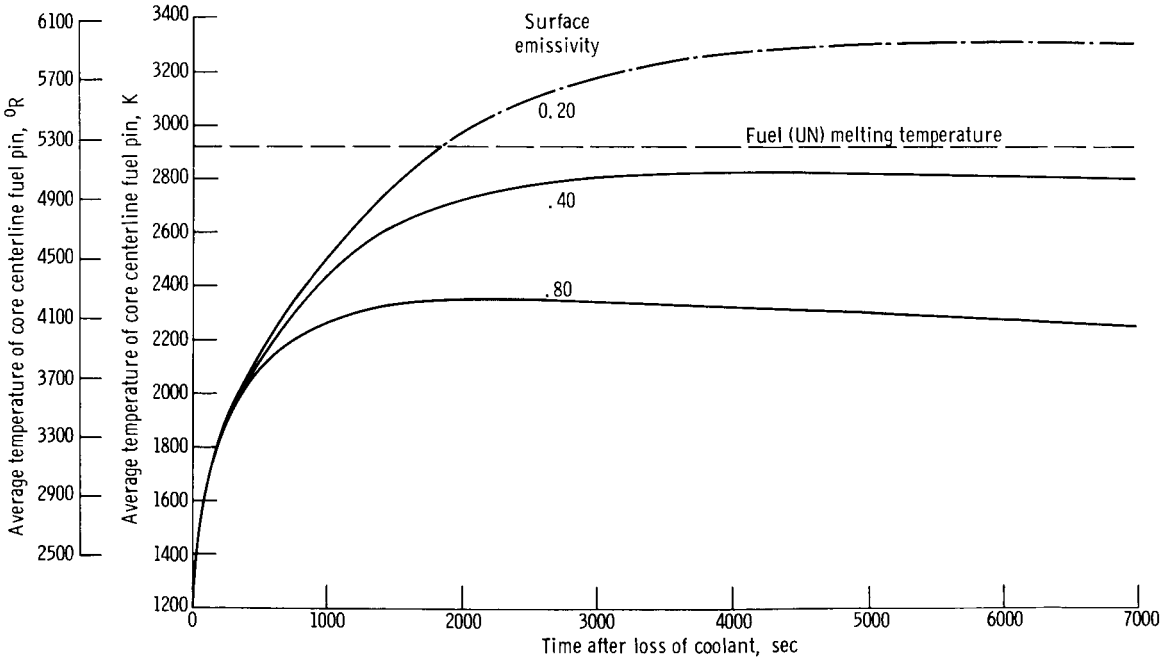

Figure 11. - Temperature of centerline fuel pin in fast-spectrum, space-power reactor against time after loss of coolant, for surface emissivities of 0.20, 0.40, and 0.80.

be recognized, however, that the dashed portion of this curve is not realistic. At the melting point, the analytical model for heat transfer breaks down due to the latent heat effects accompanying a phase change and geometry changes resulting from fuel melting. Hence, the dashed portion of the 0.20 emissivity curve represents only a ficticious temperature response that would exist if melting did not take place.

The significance of the data in figure 11 is that with loss of coolant from the core, fuel melting occurs only when the surface emissivity is somewhat less than 0.40. Table IV lists the maximum temperature of the centerline fuel pin and the times required to reach these maximum temperatures for the three emissivity values. Thus, from figure 11 and/or table IV, we conclude that for emissivity values greater than about 0.40, thermal radiation to only the surrounding 4π shield is sufficient to prevent the fuel from reaching its melting point.

TABLE IV. - TEMPERATURE RESPONSE DATA OF CORE

CENTERLINE FUEL PIN

Surface emissivity	Maximum temperature of centerline fuel pin		Time to reach melting point or maximum temperature, sec
	K	^{o}R	
0.20	(a)	(a)	[b]1900
.40	2820	5080	4000
.80	2355	4240	2200

[a]Greater than fuel (UN) melting temperature, which is approxi-
2923 K (5260^{o} R).

[b]To reach melting point of UN.

Temperature response of fuel pins in main body of core. - In this section we present a brief description of the temperature response of the individual fuel pins in the main body of the core for emissivity values of 0.20, 0.40, and 0.80. The numbering scheme which defines the fuel pins and nodal points in the analytical model of the core is given in figure 5. In the discussion which follows we refer to this numbering scheme (fig. 5) to identify the fuel pins and nodal points.

Emissivity of 0.20: We have shown in the preceding section (fig. 11) that with an emissivity of 0.20, the core centerline fuel pin reaches the melting point of UN at about 1900 seconds after the loss-of-coolant accident. As we have stated, with fuel melting, the analytical model of the core is no longer applicable. Figure 12 shows the temperature response of the fuel pins in the main body of the core for the 0.20 emissivity. The temperatures in figure 12 are fuel-pin average values. That is, they are the average

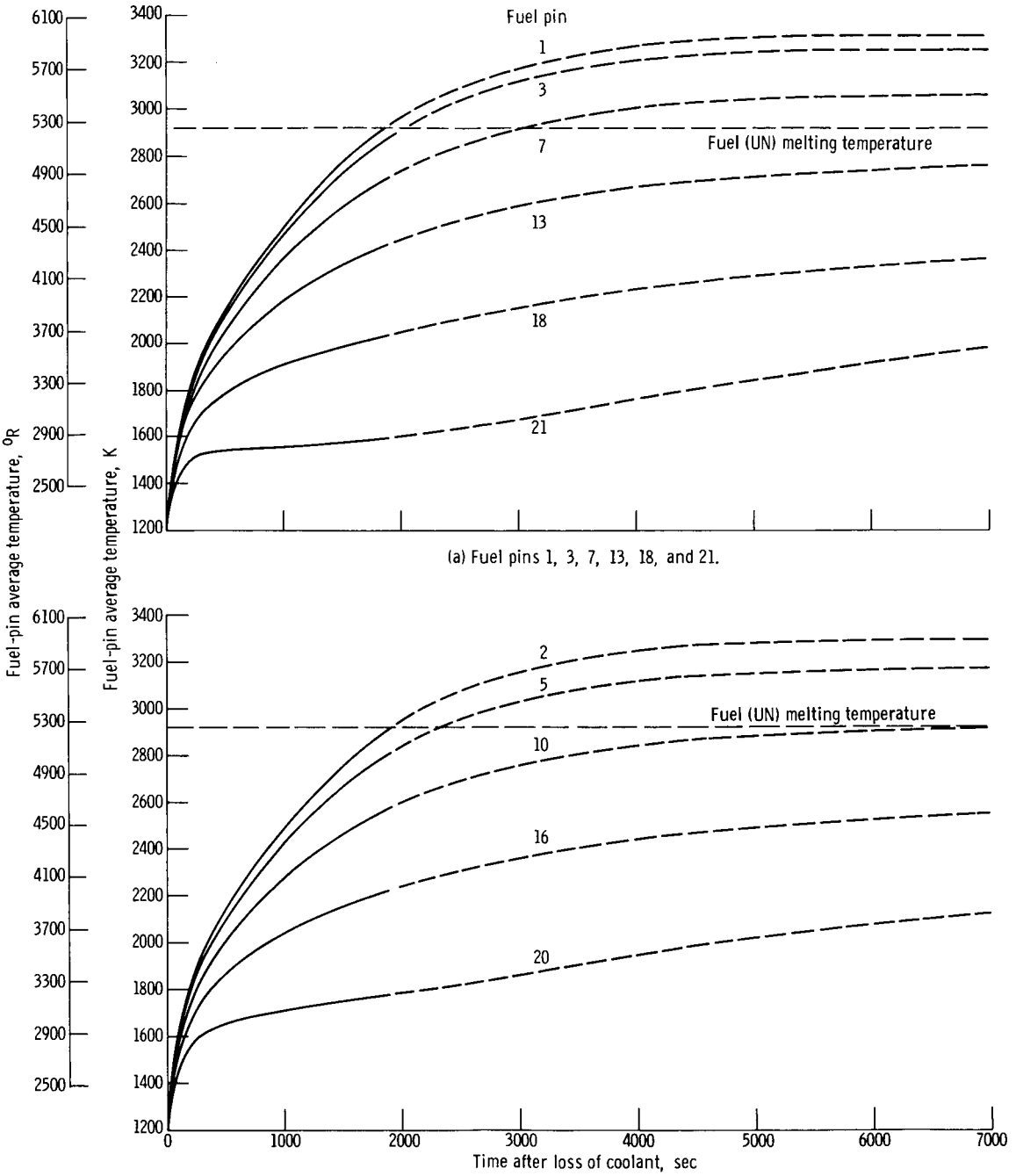

Figure 12. - Temperature response of fuel pins in main body of core following loss of reactor coolant, for emissivity of 0.20.

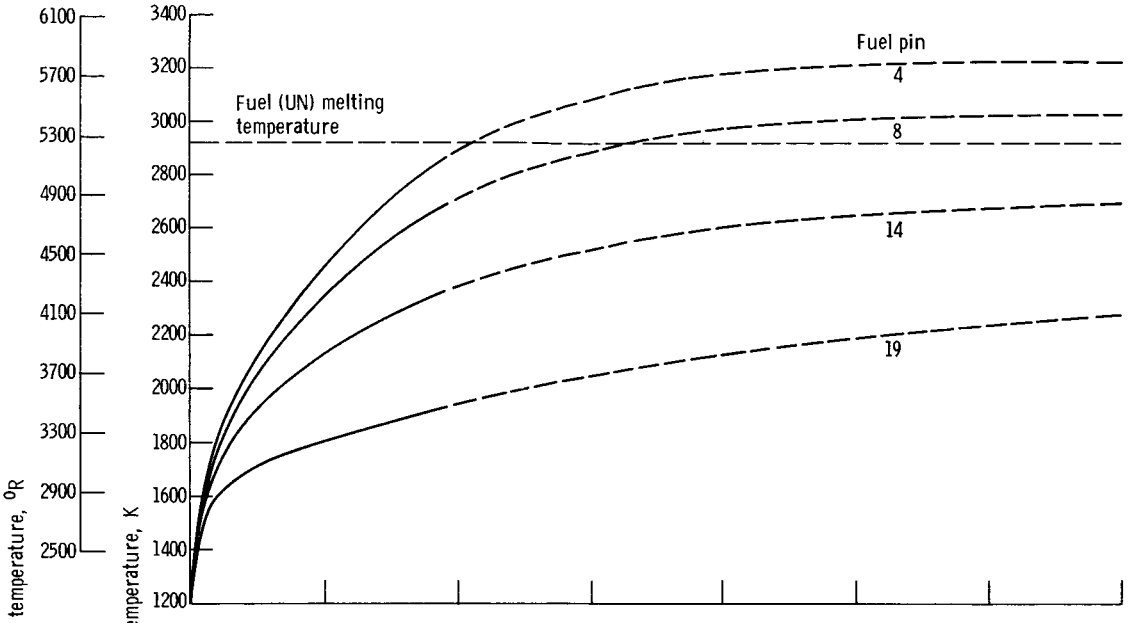

(c) Fuel pins 4, 8, 14, and 19.

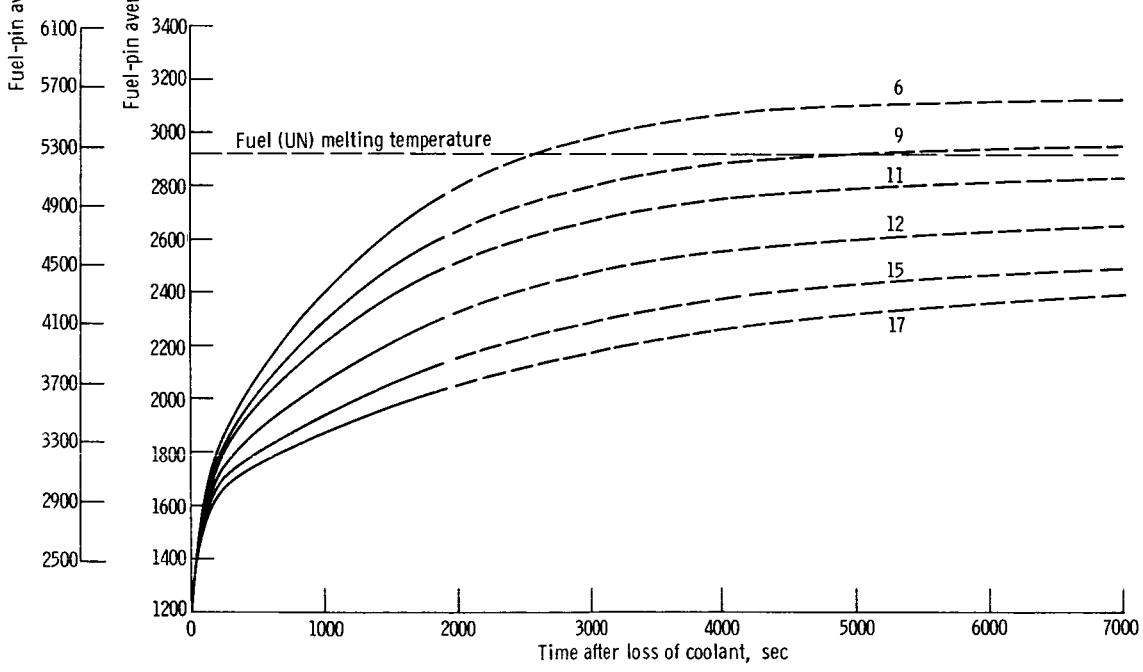

(d) Fuel pins 6, 9, 11, 12, 15, and 17.

Figure 12. - Concluded.

of the nodal point temperatures in each of the respective fuel pins. As a point of interest, with an emissivity of 0.20, the maximum temperature difference between modes associated with any single fuel pin is small - less than 20 K (36° R). However, the circumferential temperature gradient in some of the T-111 honeycomb tubes is considerably larger. At some locations in the main body of the core, the extreme temperature difference between nodes in a single T-111 honeycomb tube is as high as 220 K (396° R). For the 0.20 emissivity, all calculated temperature data beyond 1900 seconds represent only the response that would occur if there were no melting in the core. For this reason, all data curves in figure 12 are shown dashed for times greater than 1900 seconds. The spacing between curves in figure 12(a) is a measure of the radial temperature gradient in the core. From this data, we note that the radial temperature gradient between pins is relatively small near the center of the core and increases significantly with radial distance from the core center. The radial temperature gradient depicted in figure 12(a) is a characteristic of this thermal network in which the resistance to radiation heat transfer between the fuel pins increases with decreasing fuel-pin temperatures.

Emissivity of 0.40: Figure 13 shows the calculated temperature response of the fuel pins in the main body of the core based on an emissivity of 0.40. From figure 13, we note that the temperatures of all fuel pins in the main body of the core are below the melting point of UN. However, some of the fuel pins (e.g., fuel pins 1, 2, 3, and 4) reach temperatures which are within about 200 K (360° R) of the UN melting temperature. Hence, with an emissivity of 0.40, the margin between the maximum fuel-pin temperature and the melting point of UN is relatively slim, particularly for those pins in the center region of the core.

Emissivity of 0.80: With an emissivity of 0.80, the temperatures of all fuel pins in the main body of the core are considerably below the UN melting temperature. Figure 14 shows the calculated temperature response of these individual fuel pins based on an emissivity of 0.80. In figure 14, the difference between the highest fuel-pin temperature (that of fuel pin 1) and the melting temperature of UN is approximately 570 K (1026° R). Thus, with an emissivity equal to 0.80, there is a significant margin between the maximum fuel-pin temperatures and the melting temperature of UN.

In the foregoing section, we have shown the effect of emissivity on the temperature response of the individual fuel pins when only the 4π shield is considered as a heat sink. With this scheme of removing decay heat, fuel melting takes place only when the emissivity is somewhat less than 0.40. That is, for surface emissivities greater than about 0.40, thermal radiation to the surrounding 4π shield is sufficient to prevent the fuel from reaching its melting temperature.

Heat interchange between reactor and shield. - Figure 15 shows the total rate of heat transfer from the reactor to the surrounding radiation shield as a function of time after loss of coolant. For each emissivity, the rate of heat transfer decreases immediately following the loss of coolant, reaches a minimum, and then increases with time

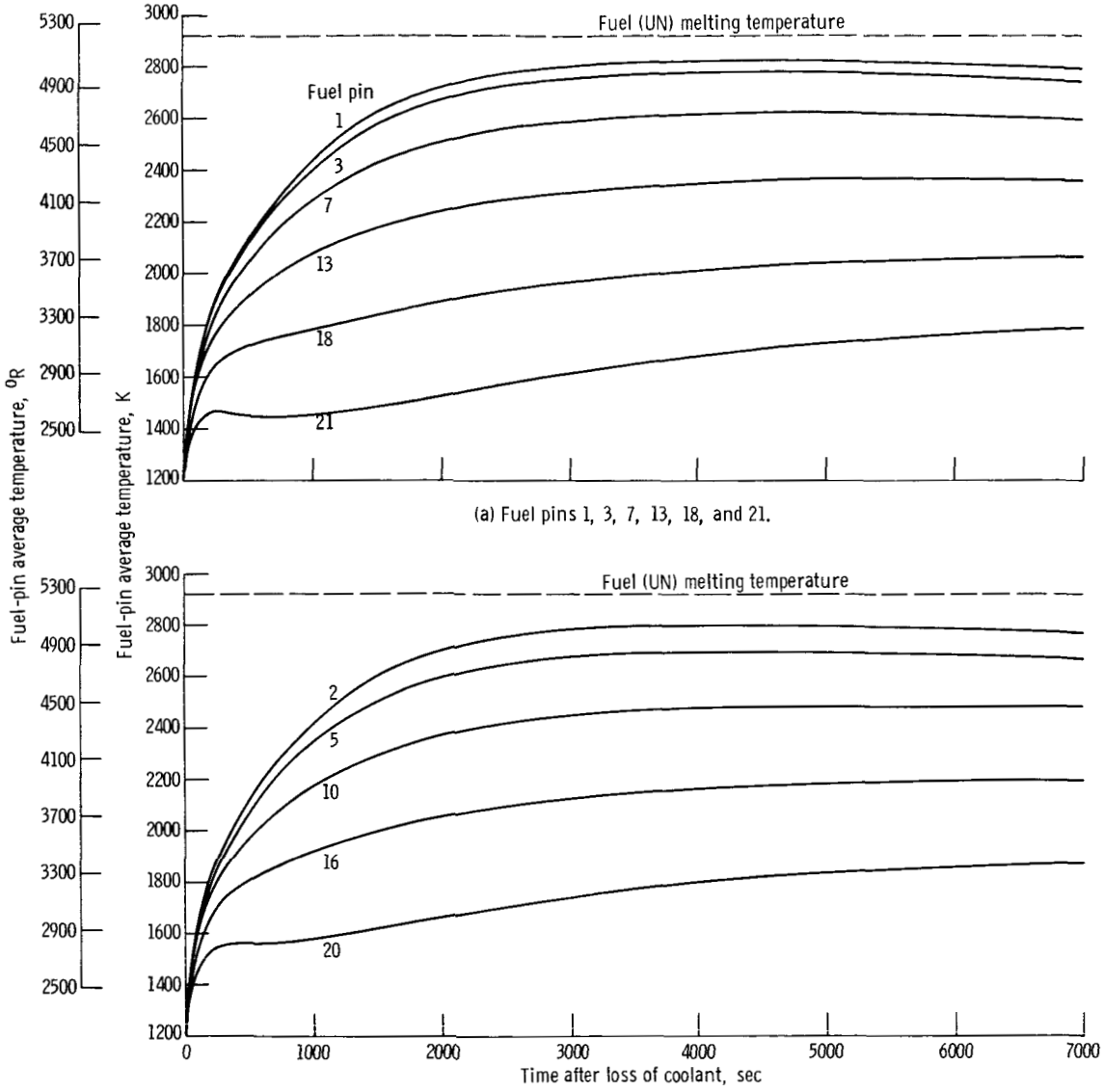

(a) Fuel pins 1, 3, 7, 13, 18, and 21.

(b) Fuel pins 2, 5, 10, 16, and 20.

Figure 13. - Temperature response of fuel pins in main body of core following loss of reactor coolant, for emissivity of 0.40.

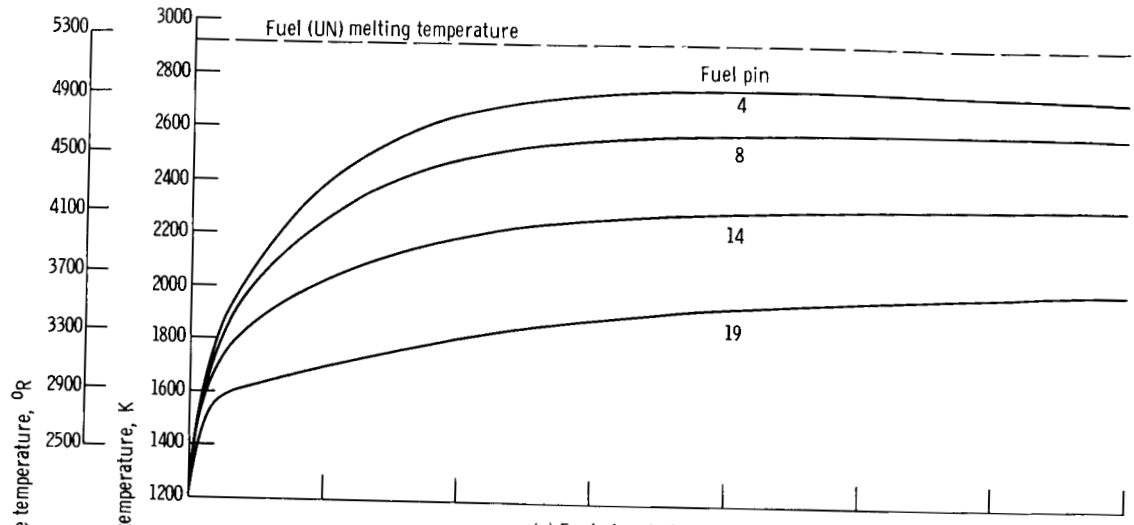

(c) Fuel pins 4, 8, 14, and 19.

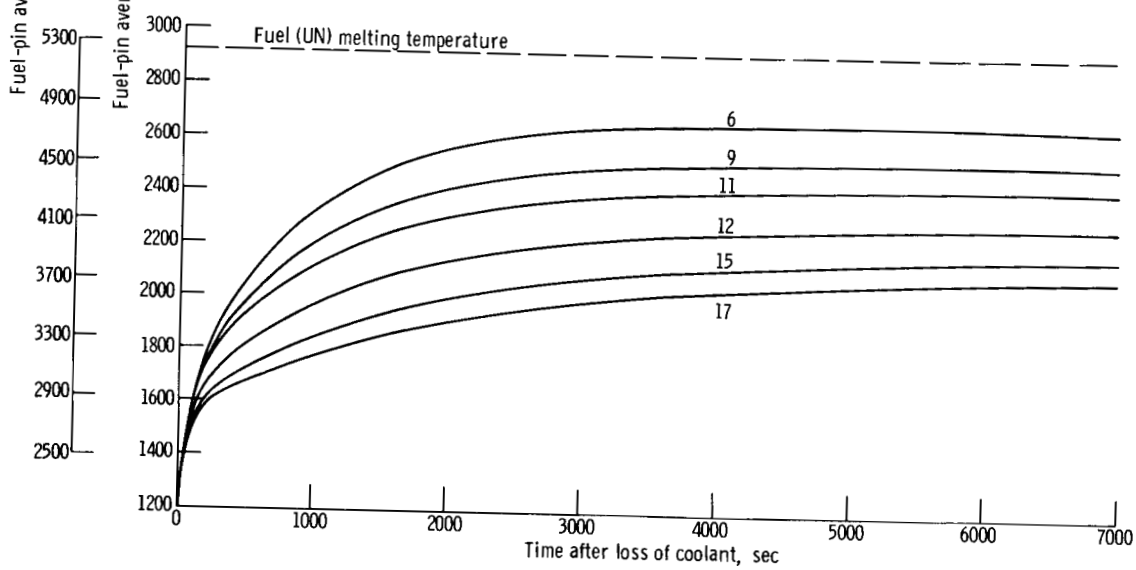

(d) Fuel pins 6, 9, 11, 12, 15, and 17.

Figure 13. - Concluded.

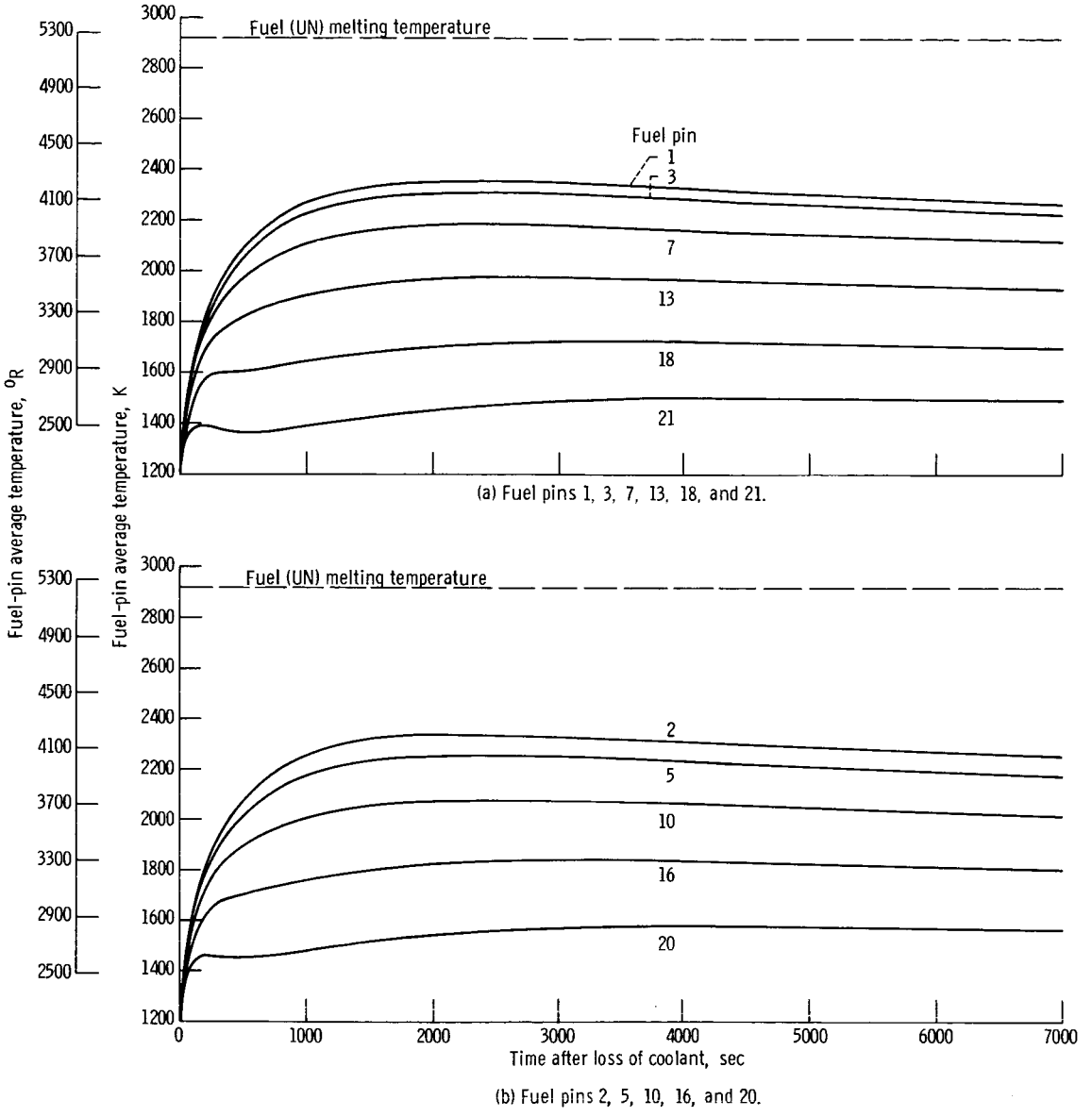

(a) Fuel pins 1, 3, 7, 13, 18, and 21.

(b) Fuel pins 2, 5, 10, 16, and 20.

Figure 14. - Temperature response of fuel pins in main body of core following loss of reactor coolant, for emissivity of 0.80.

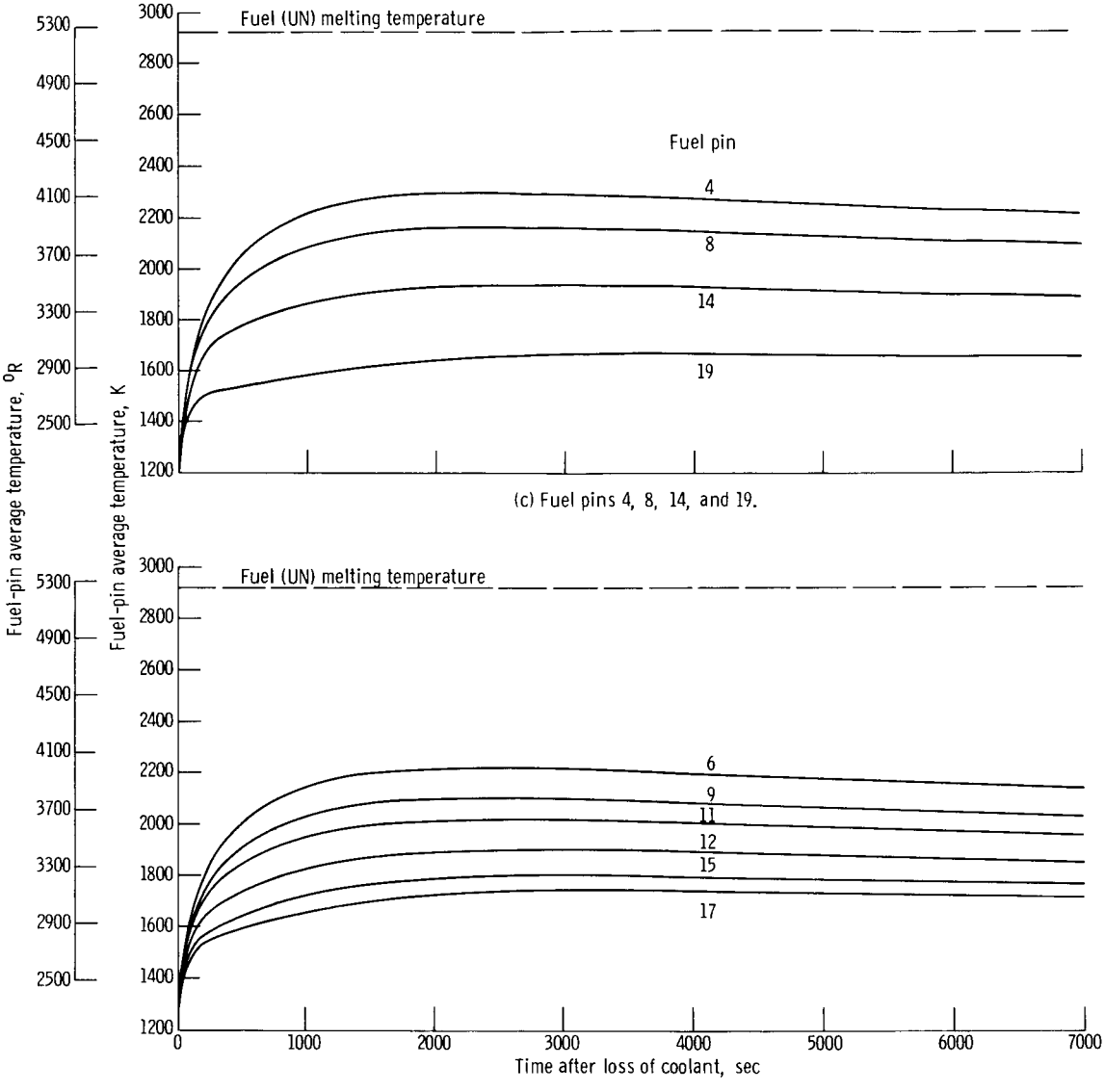

(c) Fuel pins 4, 8, 14, and 19.

(d) Fuel pins 6, 9, 11, 12, 15, and 17.

Figure 14. - Concluded.

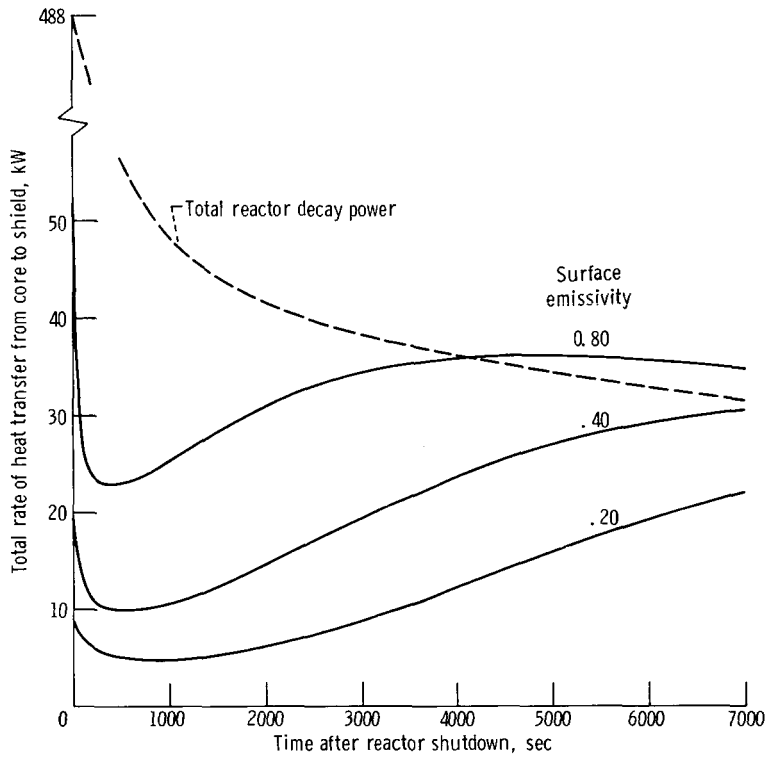

Figure 15. - Total rate of heat transfer from core to shield against time after loss of coolant for surface emissivities of 0.20, 0.40, and 0.80.

and approaches a relative maximum. Also shown in figure 15 is a dashed curve which represents the total rate of decay heat generation for this reactor against time after the loss of coolant. The difference between the total decay heat generation rate and the total rate of heat transfer from the core is the rate of thermal energy storage in the core.

A significant point of figure 15 is that the thermal capacitance of the core (and hence the average core temperature) continues to increase until the total decay power is equal to the total rate of heat transfer from the core, that is, until the respective curves intersect. Figure 15 shows that with an emissivity of 0.80, the curves intersect at about 4200 seconds. But with emissivities of 0.40 and 0.20, intersections occur at times greater than 7000 seconds. Thus, with the 4π radiation shield as the only sink for heat removal from the core, a large fraction of the decay power goes toward increasing the thermal capacitance of the core.

Scheme II - Decay Heat Absorption by Both a Redundant Coolant Channel and the Surrounding 4π Shield

In this scheme, decay heat generated in the core is transferred to both the redundant coolant channel at the center of the core and the 4π radiation shield which surrounds the core. The redundant coolant channel has a outside diameter of 2.16 centimeters (0.85 in.), which is the same as that of the honeycomb tubes. For this scheme, we used a constant sink temperature of 1222 K (2200° R) for the core centerline coolant passage and a constant sink temperature of 700 K (1260° R) for the radiation shield.

Temperature response of fuel pins in main body of core. - Figure 16 shows the temperature response of the fuel pins in the main body of the core for this scheme of decay heat removal. The data shown in this figure were calculated based on an emissivity value of 0.20. As indicated in figure 16, the temperatures of all fuel pins in the main body of the core are below the melting point of UN. The highest fuel temperature (that of fuel pin 5) is approximately 2840 K (5100° R), or about 90 K (160° R) less than the melting temperature of UN.

A comparison of the data in figures 16 and 12 shows that the addition of a redundant cooling channel at the center of the core results in a substantial decrease in the fuel-pin maximum temperatures. Even with an emissivity value as low as 0.20, the temperatures of all fuel pins remain below the melting temperature of UN.

Heat-transfer rates to centerline cooling passage and surrounding 4π shield. - Figure 17 shows the rates of heat transfer to both the centerline cooling passage and the surrounding 4π shield against time after loss of coolant. The total rate of heat removal from the core is the sum of the individual rates represented by the solid curves in this figure.

The dashed curve in figure 17 represents the total rate of decay heat generation in the reactor. From this figure, we see that the rate of heat removal by the centerline cooling channel is small in relation to the total decay power. Nevertheless, it is sufficient to prevent the temperatures of the fuel pins from reaching the melting temperature of UN, even with an emissivity value of 0.20.

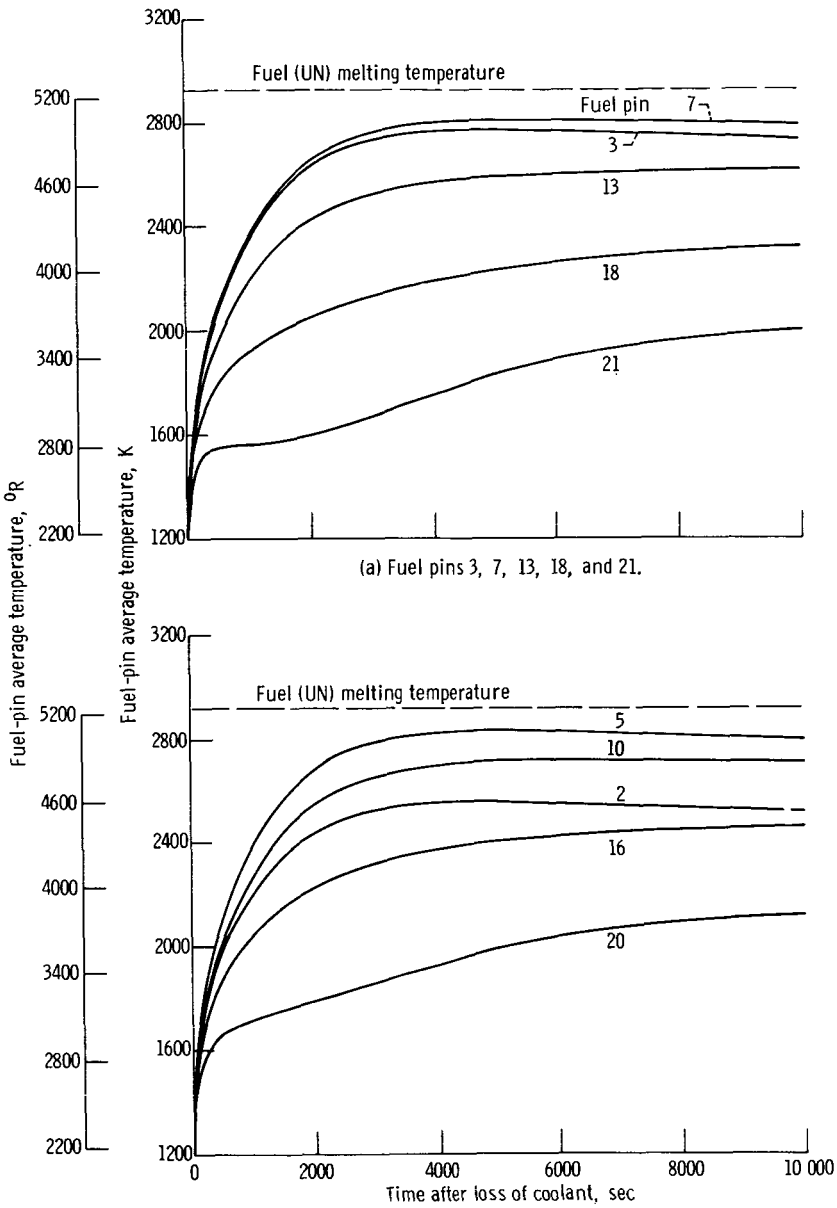

(a) Fuel pins 3, 7, 13, 18, and 21.

(b) Fuel pins 2, 5, 10, 16, and 20.

Figure 16. - Average temperatures of fuel pins in fast-spectrum space-power reactor against time after loss of coolant, with heat transfer to both core centerline coolant channel and surrounding 4π shield. Emissivity, 0.20.

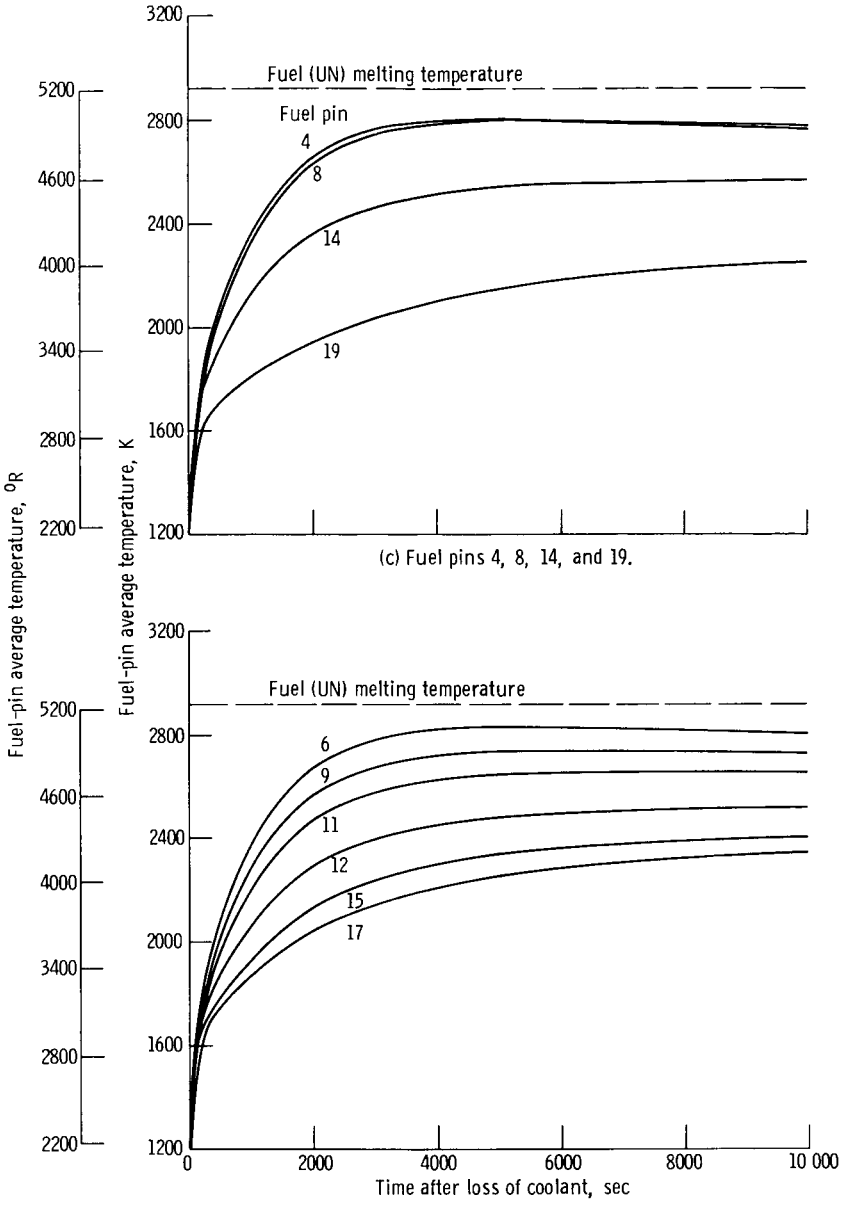

(c) Fuel pins 4, 8, 14, and 19.

(d) Fuel pins 6, 9, 11, 12, 15, and 17.

Figure 16. - Concluded.

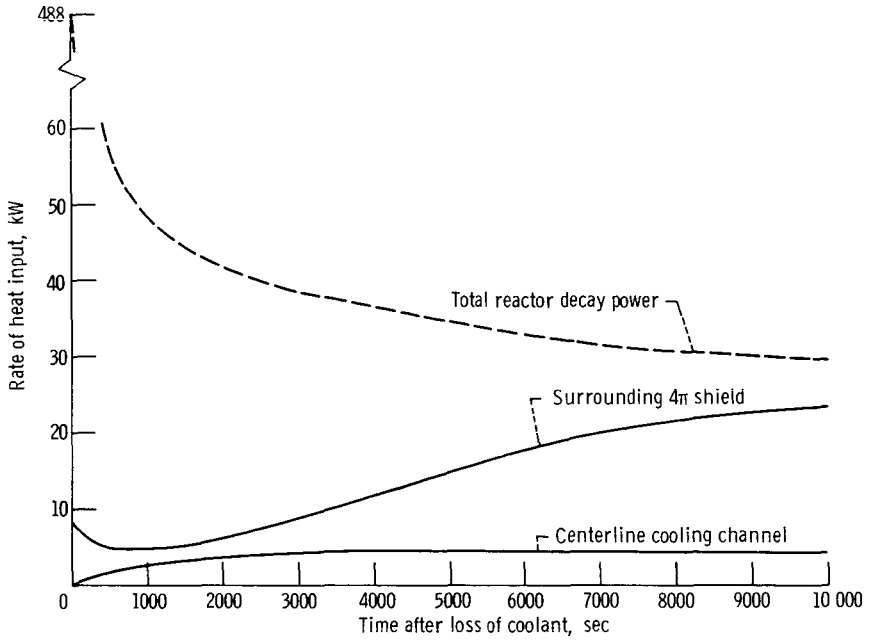

Figure 17. - Total rates of heat input to core centerline cooling passage and surrounding 4π shield against time after loss of reactor coolant. Emissivity, 0.20.

SUMMARY OF RESULTS

A two-dimensional, transient, heat-transfer analysis was made to determine the temperature response in the core of a conceptual space-power nuclear reactor following a total loss of reactor coolant. For this analysis, we assumed that (1) the reactor was operative continuously at design power (2.17 MW) for 1 year prior to the loss of coolant and (2) the reactor was shut down immediately following the loss of coolant. With loss of coolant from the reactor, the controlling mode of heat transfer is thermal radiation.

In one of the schemes considered for removing decay heat from the core, we assumed that the 4π shield which surrounds the core acts as a constant-temperature sink (temperature, 700 K (1260° R)) for absorption of thermal radiation from the core. Results based on this scheme of decay heat removal show that the surface emissivity has a significant effect on the temperature response of the core. With an emissivity of 0.20, the core centerline fuel pin reached the melting temperature of UN (2923 K, or 5260° R) at about 1900 seconds after the loss-of-coolant accident. And with emissivity values of 0.40 and 0.80, the maximum fuel-pin temperatures were 2820 K (5080° R) and 2355 K (4240° R), respectively. Thus for emissivity values greater than about 0.40, thermal radiation to only the surrounding 4π shield is sufficient to prevent the fuel from reaching its melting point.

In another scheme for removing decay heat, the centerline fuel pin was replaced by a redundant coolant channel. With this arrangement, decay heat generated in the core

is transferred to both the redundant coolant channel at the center of the core and the 4π radiation shield which surrounds the core. A constant temperature of 1222 K (2200° R) was assumed for the redundant coolant channel, and the 4π shield temperature was assumed constant at 700 K (1260° R).

Based on a surface emissivity of 0.20 for all core materials, the calculated maximum fuel temperature for this scheme of heat removal was 2840 K (5100° R), or about 90 K (160° R) less than the melting temperature of UN. Hence, it appears that a single coolant channel at the center of the core is sufficient to prevent fuel melting, even with a surface emissivity value as low as 0.20.

Lewis Research Center,
National Aeronautics and Space Administration,
Cleveland, Ohio, October 8, 1971,
112-27.

APPENDIX - SYMBOLS

A	cross-sectional area for conduction, m^2; ft^2
A_s	surface area, m^2; ft^2
C_p	specific heat, kW-sec/(kg)(K); Btu/(lbm)(^oR)
F	configuration factor for radiation heat transfer
G_C	conductor conductance, kW/K; Btu/(sec)(^oR)
G_R	radiation conductance, kW/K^4; Btu/(sec)$(^oR)^4$
k	thermal conductivity, kW/(m)(K); Btu/(sec)(ft)(^oR)
l	characteristic length between conductor nodes, m; ft
q'''	volumetric heat generation rate, kW/m^3; Btu/(sec)(ft^3)
T	temperature, K; ^oR
V	volume, m^3; ft^3
ϵ	emissivity
θ	time, sec
ρ	density, kg/m^3; lbm/ft^3
σ	Stefan-Boltzmann constant, 5.71×10^{-11} $kW/(m^2)(K^4)$; 0.476×10^{-12} Btu/(sec)$(ft^2)(^oR)^4$

Subscripts:

d, e, f, g, i, j, k, l	nodal designations (fig. 5 and/or fig. 8)
α	general nodal point designation
β	general nodal point designation
θ_1	time at beginning of time period $(\theta_2 - \theta_1)$
θ_2	time at end of time period $(\theta_2 - \theta_1)$

REFERENCES

1. Whitmarsh, Charles L., Jr.: Neutronic Design for a Lithium-Cooled Reactor for Space Applications. NASA TN D-6169, 1971.

2. Turney, George E.; Kieffer, Arthur W.; and Petrik, Edward J.: Operating Characteristics of the Primary Flow Loop of a Conceptual Nuclear Brayton Space Powerplant. NASA TM X-2161, 1971.

3. Davison, Harry W.: Preliminary Analysis of Accidents in a Lithium-Cooled Space Nuclear Powerplant. NASA TM X-1937, 1970.

4. Lewis, D. R.; Gaski, J. D.; and Thompson, L. R.: Chrysler Improved Numerical Differencing Analyzer for 3rd Generation Computers. Rep. TN-AP-67-287, Chrysler Corp. (NASA CR-99595), Oct. 20, 1967.

5. Lyman, Taylor, ed.: Properties and Selection of Metals. Vol. 1 of Metals Handbook. Eighth ed., American Society for Metals, 1961, p. 1223.

6. Rough, F. A.: Properties of Fuels for Compact Nuclear Space Reactors LOG-CO-4078. Battelle Memorial Inst., Sept. 10, 1966.

7. Goldsmith, Alexander: Thermophysical Properties of Solid Materials. Vol. 1. Armour Research Foundation, Aug. 1960.

8. Wolf, J., ed.: Aerospace Structural Metals Handbook. Vol. II. Non-Ferrous Alloys. Belfour Stulen, Inc. (AFML-TR-68-115), 1971.

NASA-Langley, 1972 —— 22 E-6571